NASA/TM—1998-208402 AIAA–98–3119

Energy Efficient Engine Low Pressure Subsystem Aerodynamic Analysis

Edward J. Hall, Robert A. Delaney, and Sean R. Lynn
Allison Engine Company, Indianapolis, Indiana

Joseph P. Veres
Lewis Research Center, Cleveland, Ohio

Prepared for the
34th Joint Propulsion Conference and Exhibit
cosponsored by AIAA, ASME, SAE, and ASEE
Cleveland, Ohio, July 13–15, 1998

National Aeronautics and
Space Administration

Lewis Research Center

July 1998

Acknowledgments

The work described in this paper was supported under the NASA High Performance Computing and Communication Program (HPCCP), contract NAS3–27394, Task 13.

Available from

NASA Center for Aerospace Information
7121 Standard Drive
Hanover, MD 21076
Price Code: A03

National Technical Information Service
5287 Port Royal Road
Springfield, VA 22100
Price Code: A03

Energy Efficient Engine Low Pressure Subsystem Aerodynamic Analysis

Edward J. Hall*

Robert A. Delaney†

Sean R. Lynn‡
Allison Engine Company, Indianapolis, IN 46241

Joseph P. Veres§
NASA Lewis Research Center, Cleveland, OH 44135

The objective of this study was to demonstrate the capability to analyze the aerodynamic performance of the complete low pressure subsystem (LPS) of the Energy Efficient Engine (EEE). Detailed analyses were performed using three-dimensional Navier-Stokes numerical models employing advanced clustered processor computing platforms. The analysis evaluates the impact of steady aerodynamic interaction effects between the components of the LPS at design and off-design operating conditions. Mechanical coupling is provided by adjusting the rotational speed of common shaft-mounted components until a power balance is achieved. The Navier-Stokes modeling of the complete low pressure subsystem provides critical knowledge of component aero/mechanical interactions that previously were unknown to the designer until after hardware testing.

Nomenclature

A	Area
A_{total}	Total area
$ADPAC$	Advanced Ducted Propfan Analysis Code
BPR	Bypass ratio
CAS	Computational AeroSciences
Cl	Climb
CFD	Computational Fluid Dynamics
Cr	Cruise
EEE	Energy Efficient Engine
LE	Leading Edge
LP	Low Pressure
LPS	Low Pressure Subsystem
HP	High Pressure
N	Corrected Speed
$NPSS$	Numerical Propulsion System Simulation
O/L	Operating line
P	Pressure, psia
SLS	Sea level static
T	Temperature, degrees R
TE	Trailing Edge
V	Velocity, ft/s
c_0	Speed of sound
rpm	Revolutions per minute
u	Axial velocity
x, r, θ	cylindrical body axes
x, y, z	Cartesian body axes
ρ	Density, kg/m^3

Subscripts

$exit$	exit value
$inlet$	inlet value
s	static quantity
t	total (stagnation) quantity

Introduction

COMPETITIVE market conditions in the gas turbine industry have placed stringent demands on engine manufacturers to respond to customer requirements with efficient, cost effective products with significant reductions in development time. During the engine development period, component efficiencies often fall short of desired goals by significant margins. The engine cycle rebalance which results causes other components to operate at non-optimal (off-design) flow conditions, further reducing efficiency and complicating the identification of the original source of inefficiency. Expensive, multiple build rig testing, representing a major portion of the overall development cost, has, in the past, been required to balance component performance and optimize the engine system design.

*Staff Research Scientist, Advanced Turbomachinery Dept., Member AIAA

†Chief, Advanced Turbomachinery Dept., Senior Member AIAA

‡Advanced Turbomachinery Dept., Member AIAA

§Manager, Engine Systems, Computer and Interdisciplinary Systems Office, Member AIAA

Efforts to attack the problems associated with aircraft gas turbine engine development have been addressed through several NASA Programs. The Advanced Subsonic Technology (AST) Program specifically supports technology development to improve the performance of subsonic aircraft, both in flight characteristics and propulsion. The High Performance Computing and Communication (HPCC) Program and more specifically, the Computational Aerosciences (CAS) Project are directed to accelerate the availability of high performance computing technology for use by the U.S. aerospace community. A "Grand Challenge" application under the HPCCP is the high fidelity, interdisciplinary simulation of a full propulsion system, called the Numerical Propulsion System Simulation (NPSS).

Component design teams depend on numerical analysis techniques to achieve the best performance. Streamline curvature methods continue to be extensively used to analyze multistage turbomachinery. More recently, the trend has been to apply advanced 2-D and 3-D numerical techniques[1] to engine components to understand the details of their operation in isolation. Multistage analyses for turbomachinery are also becoming increasingly more valuable,[2].[3]

These advanced component analysis techniques often do not systematically account for inter-component interactions. Multistage analyses may someday provide adequate representation of interaction effects between blade rows in an axial compressor, for example, but do not presently provide information related to inter-component interactions (HP/LP turbine systems, e.g.). This paper describes efforts directed at creating a system which will allow individual component models to be coupled to create a full engine simulation.

Energy Efficient Engine

In 1976 NASA initiated the Aircraft Energy Efficiency (ACEE) Program to assist in the development of technology for more fuel-efficient aircraft for commercial airline use. The Energy Efficient Engine (EEE) Project of the ACEE Program was intended to lay the advanced technology foundation for a new generation of turbofan engines. This seven-year cooperative government-industry effort, was aimed at developing and demonstrating advanced component and systems technologies for engines that could be introduced into airline service by the late 1980's or early 1990's. Under the EEE Program, both isolated component and engine rig tests were performed based on a demonstrator engine developed by the General Electric Corporation, which has since come to be known simply as the Energy Efficient Engine (all further references in this document for EEE shall refer to the engine, not the ACEE EEE Program, per se). The EEE provides a natural vehicle for the type of large scale simulation developed for this study due to the availability of both subcomponent test rig data, as well as fully coupled, assembled engine test data.

Objectives of this Study

The overall objective of this project is to provide the capability to analyze the aerodynamic performance in the complete low pressure subsystem (LPS) of the Energy Efficient Engine (EEE) using three-dimensional Navier-Stokes numerical models. The analysis evaluates the impact of steady aerodynamic interaction effects between the components of the LPS at the design and at off-design operating conditions. The approach for creating the LPS model was to select a validated Navier-Stokes (N-S) analysis code, and create the EEE LPS model from the geometric components in the LPS including: external flow, nacelle, inlet, fan blades, bifurcated bypass and core inlet, bypass vanes, core inlet guide vanes, quarter height booster stage, low pressure turbine blades, mixer, and exhaust nozzle. Engine core components were modeled using appropriate boundary conditions derived from test data and an engine cycle performance deck. The N-S analysis of the fully coupled LPS enables a torque balance on the low pressure spool at quasi-steady state operating conditions.

This study was divided into five major milestone areas:

- **Geometry Definition:** Detailed geometry definitions of the components of the Energy Efficient Engine primary gas flowpaths were assembled.
- **Mesh Generation:** Geometry definitions described above were employed to develop discrete mesh systems suitable for CFD analysis.
- **Component Validation Study:** Block components of the LP and HP subsystems were analyzed using CFD tools to verify the accuracy of the geometry definitions, and to validate the CFD analysis with available rig test data.
- **LP Subsystem Analysis:** Various components were assembled to form the discrete representation of the LP Subsystem, and a quasi-steady CFD analysis was applied to predict both the aerodynamic and mechanical coupling of the LP Subsystem.
- **Core Cycle Specification:** An engine cycle performance model was coupled with the 3-D CFD analysis to represent the operating parameters for the engine core in the LP Subsystem Analysis.

Each of the five milestone topics are described in more detail in the sections which follow. The ultimate objective of this study was to develop a simulation capability for the LP Subsystem of modern high bypass

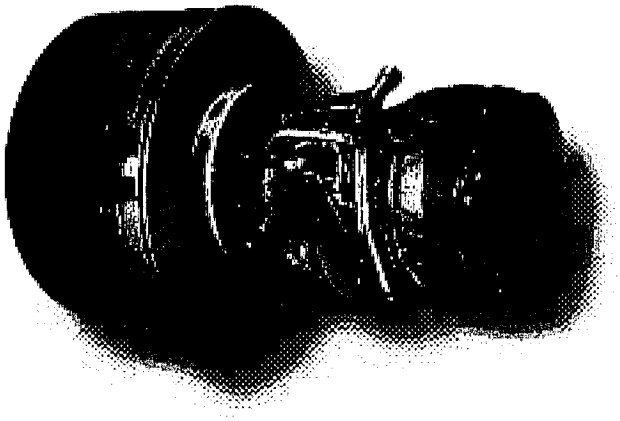

Fig. 1 Energy Efficient Engine test rig hardware.

ratio turbofan engines which would address the goals of the NASA NPSS Program.

Geometry

Detailed geometry for the EEE model was extracted from the NASA Energy Efficient Engine Master Geometry Database. This database was developed specifically for NPSS-related applications which employ the EEE design for demonstration. The database consists of NASA IGES curve-based and surface-based entities describing the major components of the engine core and bypass gas flowpaths. Exact geometric definitions of the EEE LPS are employed, with the exception of the outer nacelle and inlet, which have been designed consistent with the Energy Efficient Engine design philosophy in order to take the place of the test rig bellmouth. A picture of the Energy Efficient Engine test rig hardware is given in Figure 1.

NEPP Cycle Analysis

One facet of the analyses performed during this study was the desire to investigate aspects of the "zooming" feature of the planned NPSS engine performance analysis architecture. In this regard, the intention was to numerically couple detailed CFD simulations of the EEE LP spool with an engine cycle analysis of the EEE HP core. This coupled simulation, would, in fact, be a complete simulation of the two-spool EEE engine with varying levels of fidelity for the LP and HP subsystems. The *ADPAC* analysis was directed at the 3-D CFD portion of this simulation strategy, while the *NEPP* 1-D cycle analysis was directed at the HP spool simulation strategy.

The *NEPP* computer program[4] performs one-dimensional, steady-state thermodynamic performance analysis of aircraft gas turbine or jet engine configurations. Data inputs specify a standard set of components and their interconnections, allowing simulation of virtually any engine configuration. Physical components which may be used include propellers, inlets, ducts, combustors, fans, compressors, turbines, shafts, heat exchangers, flow splitters, subsonic mixers and/or supersonic ejectors, nozzles and water injectors or gas generators.

There are several steps for putting together a NEPP input file to analyze an engine system.

- Select the engine cycle.
- Convert the cycle into a block diagram for NEPP.
- Define the compressor and turbine performance maps. Exact maps for the application are not required, the program can scale maps as required.

ADPAC Code Description

The aerodynamic predictions for the cases described in this study were obtained using the *ADPAC* analysis code. The *ADPAC* code is a general purpose aerospace propulsion aerodynamic analysis tool which has undergone extensive development, testing, and verification.[5] Detailed code documentation is also available for the *ADPAC* program .[6]

The *ADPAC* analysis solves a time-dependent form of the three-dimensional Reynolds-averaged Navier-Stokes equations using a proven time-marching numerical formulation. The numerical algorithm employs robust numerics based on a finite-volume, explicit Runge-Kutta time-marching solution algorithm derived from the developmental efforts of Jameson et al.,[7] Adamczyk et al.,[8] and Arnone et al.[9] Several steady-state convergence acceleration techniques (local time stepping, implicit residual smoothing, and multigrid) are available to improve the overall computational efficiency of the analysis. A relatively standard implementation of the Baldwin and Lomax[10] turbulence model with wall functions was employed to compute the turbulent shear stresses and turbulent heat flux.

The *ADPAC* code permits the use of a multiple-blocked mesh discretization which provides extreme flexibility for analyzing complex geometries. The block gridding technique enables the coupling of complex, multiple-region domains with common (non-overlapping) grid interface boundaries through specialized user-specified boundary condition procedures.

ADPAC supports coarse-grained computational parallelism via block boundary-specified message passing. Interprocessor communication is controlled by the Message Passing Interface (MPI) [11] communication protocol. Both serial and parallel computations were employed during this study utilizing a wide range of high speed processors, workstation clusters, and massively parallel computing platforms, depending on availability.

Steady-state aerodynamic predictions for multistage turbomachinery are performed using a specialized boundary procedure known as a "mixing plane".[2] The

mixing plane strategy was developed to permit numerical simulations based on only a single blade passage representation for each blade row, regardless of the differences in circumferential spacing for each blade row. This simplification is afforded by circumferentially averaging data on either side of the interface between blade rows (the mixing plane), and then passing that information as a boundary condition to the neighboring blade row.

Mesh Generation

Numerous meshing strategies are possible with the *ADPAC* code, the simplest of which is simply to use a single sheared H-type mesh for each blade row (see e.g.[2]). This meshing strategy also has the direct benefit that the resulting mesh could also be used for other NPSS-related multistage turbomachinery flow analyses. A key element of the meshing strategy in this project was to employ the Master Engine Geometry Database IGES entities directly in the grid generation process. Many mesh generation codes require discretized point data as input to define the geometry of interest. This discretized definition, and the subsequent interpolations which occur during the mesh generation process can lead to errors in the coordinates of the final mesh. One focus of the NPSS geometry definition has been to employ analytical definitions of geometric components in the form of IGES or NURBS-based entities. These analytical definitions would then form a consistent geometric database for all disciplines (aerodynamic, stress, heat transfer, etc.) and significantly reduce errors due to interpolations and interpretations of discrete point data. In order to address the mesh objectives described above, a procedure to generate meshes for the EEE LPS analysis directly from the NASA Energy Efficient Engine Master Engine Geometry Database was developed and is described in the paragraphs below.

The construction of the numerical mesh system for each individual component is performed in a manner which permits a simple coupling of the component meshes for the complete LPS analysis. H-type computational meshes are employed for this purpose, although the analysis need not be limited in this fashion. A primary focus of the NPSS research is to employ a consistent geometry definition during all phases of the engine analysis. As such, a mesh generation strategy was developed whose only direct geometric input is the NASA-IGES based geometry of the Master Engine Geometry Database. A graphical illustration of the mechanics of the mesh generation procedure is given in Figure 2.

The procedure is initiated by defining the exact geometric axial extents of the blade elements in the axisymmetric projection of the flowpath. This procedure was accomplished by interrogating the geometric elements for each individual blade row, and extracting the geometric leading and trailing edge outlines (in this sense, the geometric leading and trailing edges are represented by the minimum and maximum axial coordinate locations, respectively). In essence, the radial profiles of the blade minimum and maximum axial coordinates were extracted from the blade IGES surface definition. These new entities are themselves represented in *GRIDGEN* database segment format and are added to the geometry database.

Once the blade row extents are defined, standard NASA-IGES capable mesh generation schemes

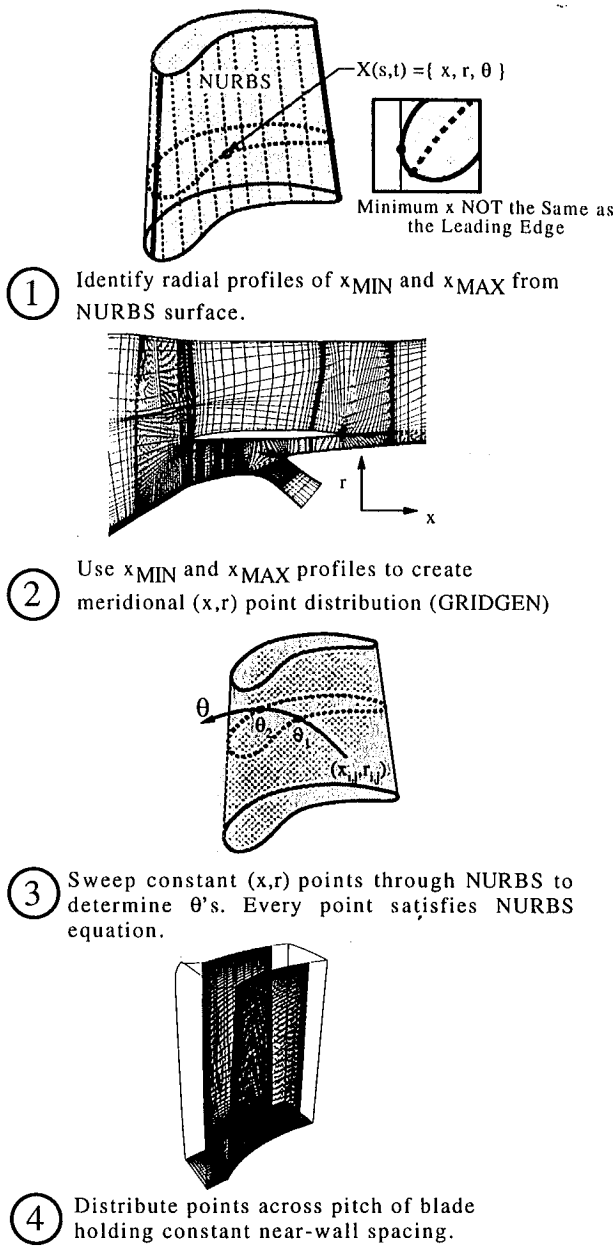

Fig. 2 Component mesh generation procedure for EEE LPS analysis.

(GRIDGEN[12] was used for this exercise) can be employed to define the meridional projection of the H-type meshes. The blade leading and trailing edge elements define the positions of the blade rows in the axisymmetric projection, while the Master Engine Geometry Database flowpath definitions define the endwalls. The *GRIDGEN* program (which can read in the IGES entities as a geometry database) is then used to define the axial (x) and radial (r) point distributions in the meridional projection. Typical mesh dimensions for the axisymmetric components of the meshes employed 49 points radially along the blade span, and 65 points axially along the chord of the blade.

Next, the (x, r) coordinate pairs from the meridional mesh projection are swept through the airfoil IGES surface definition to determine the blade surface circumferential (θ) point distributions. The remaining points in the circumferential direction (between airfoils) are defined using a simple hyperbolic distribution routine (see e.g. [13]). The circumferential distributions were constructed to maintain a fixed, specified near wall spacing in the circumferential direction. Most of the mesh generation procedure is automated, though some hand construction was unavoidable. A complete mesh for a compressor or turbine subcomponent, for example, generally required 4 hours to complete.

Component Validation Study

Component performance validation was considered a necessary milestone both in validating the accuracy of the analysis as well as verifying the accuracy of the geometry specifications in the EEE Master Engine Geometry Database. During this phase of the program, specific subcomponent geometries were selected and analyzed in isolation from the other major subcomponents of the overall EEE LPS analysis.

EEE Fan Section Analysis

The EEE fan section design is based on a unique split flow configuration selected to minimize mission fuel burn and direct operating cost. An illustration of the EEE fan section flowpath and blade arrangement is given in Figure 3. The EEE fan section design employs a full span fan rotor with a design corrected tip speed of 1350 ft/s. and an inlet radius ratio of 0.342. The fan employs a part span shroud to improve structural rigidity. The fan rotor exit flow is split radially by an island splitter. The inner annulus of this island splitter is designed to capture 22% of the fan flow and employs a 1/4-height booster stage. The 1/4-height booster stage further supercharges the flow entering the core and enhances core protection from foreign object damage. The use of the booster stage also permits a lower fan rotational speed, increased fan efficiency, lower fan hub aerodynamic loading, and provides for an easier engine growth path. The flow through the booster stage is subsequently split by the core inlet,

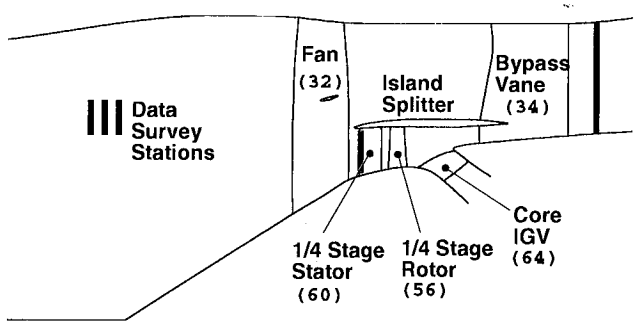

Fig. 3 Axisymmetric projection of EEE fan+1/4-height booster stage configuration ilustrating test data instrumentation plane locations.

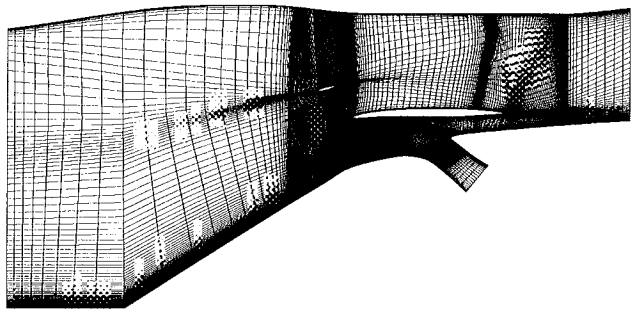

Fig. 4 Axisymmetric projection of EEE fan section multi-block H-type mesh system.

with 68% of the booster flow entering the core and the remaining 42% of the booster flow reentering the bypass flowpath through the bypass vane. The outer annulus flow carries the remaining 78% of the fan rotor flow through the bypass vanes. The analysis included the full height fan with part span shroud, 1/4-height booster stage, core inlet guide vane, and bypass vane as shown in Figure 3.

The mesh generation procedure previously described was employed to define a 1,605,000 cell mesh distributed among 8 mesh blocks. An illustration of the axisymmetric projection of the mesh system is given in Figure 4.

A design point analysis was performed for the EEE fan section using the mesh system described in the previous subsection. The EEE fan section design bypass ratio is 6.8, and the fan design point represents the engine maximum climb operating point. The analysis was performed on a 4-processor Silicon Graphics Power Challenge L multiprocessor computer with 1 GB of main memory. A converged solution was obtained in a total of 6 hours (wall clock time) using all four processors. Figure 5 illustrates the predicted fan surface static pressure contours from the analysis. Numerical predictions for the EEE fan section were compared with experimental data derived from full scale rig tests of the fan section.[14] Figure 6 illustrates a comparison of predicted and experimental bypass vane exit and 1/4-stage vane leading edge spanwise total pres-

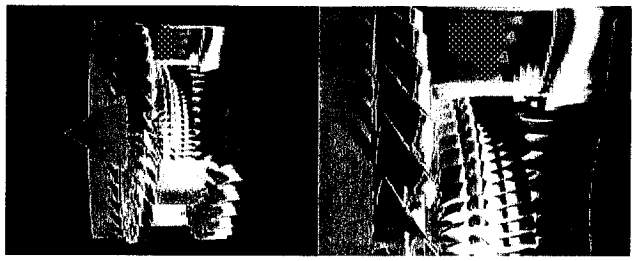

Fig. 5 Predicted surface static pressure contours for EEE fan plus 1/4-height booster stage configuration.

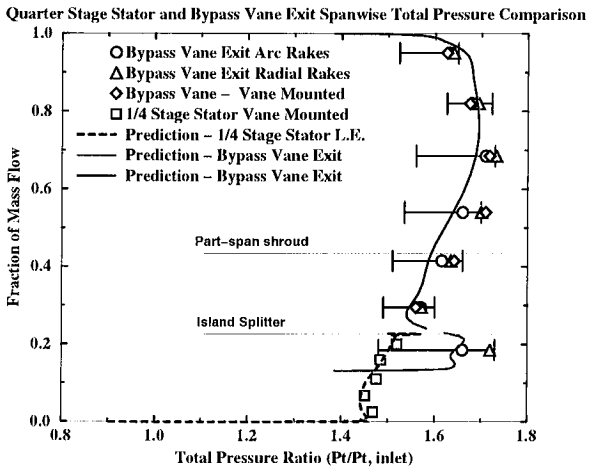

Fig. 6 Comparison of predicted and experimental spanwise total pressure distributions at bypass vane exit and 1/4-stage vane leading edge for EEE fan plus 1/4-height booster stage configuration.

sure distributions. The total pressure distributions are plotted and correlated with the colors of the data survey stations indicated on Figure 3. The character of the spanwise pressure distribution was very accurately captured, and was well within the range of the test data.

In order to investigate the off-design analysis capabilities of the EEE fan section model, a number of predictions were performed at 100% corrected speed with variations in both fan exit static pressure and fan section bypass ratio. These off-design results were obtained by prescribing the flow entering the core, and adjusting the bypass exit static pressure until the desired fan inlet flow was achieved. Excursions in predicted bypass ratio ranged from 6.0 to 10.8.

Predictions of overall performance were compared with measured data derived from full-scale rig tests of the fan section.[14] A comparison of predicted and experimental overall pressure ratio and adiabatic efficiency versus corrected mass flow rate for the core stream flow (downstream of the core inlet guide vane) of the EEE fan section is given in Figure 7. The

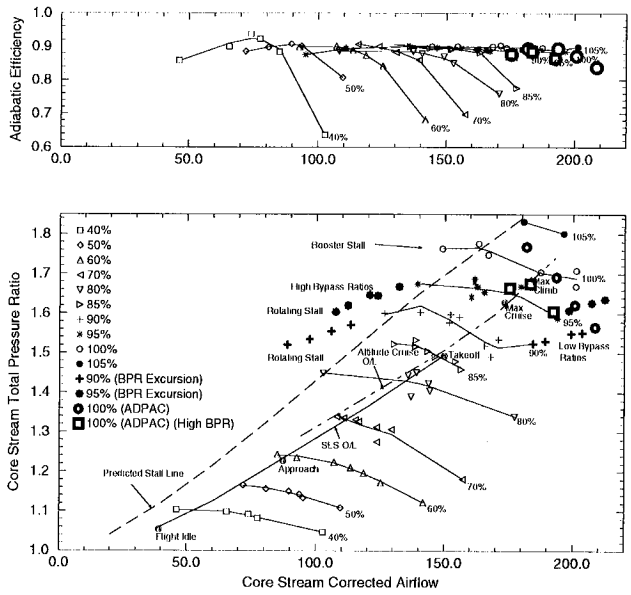

Fig. 7 Comparison of predicted and experimental total pressure ratio and adiabatic efficiency versus corrected flow rate for the core inlet of the EEE fan section.

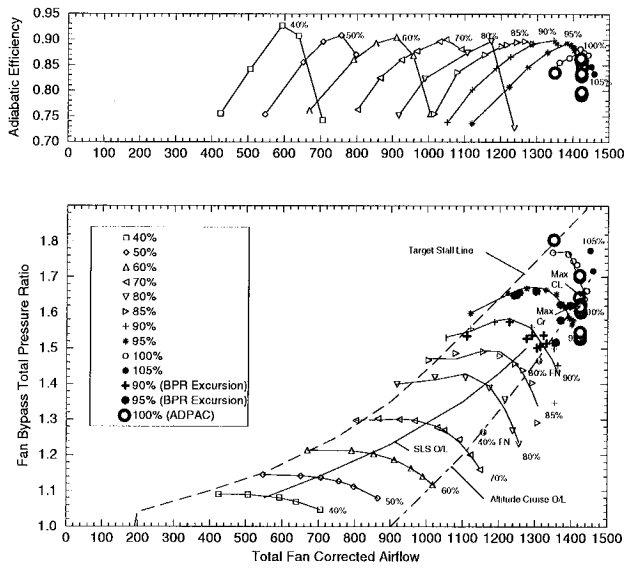

Fig. 8 Comparison of predicted and experimental total pressure ratio and adiabatic efficiency versus corrected flow rate for the bypass duct flow of the EEE fan section.

corresponding maps for the fan bypass stream flow (downstream of the fan bypass vane) is given in Figure 8. The data on these figures illustrates the overall capabilities of the EEE fan design. Bold symbols on each figure illustrate the test performance at extreme high and low values of bypass ratio. It is interesting to note that in both the test and the prediction, bypass ratio did not significantly alter the characteristics of the bypass stream, but does have a significant ef-

fect on the core stream flow. The overall character of the off-design performance predictions displayed good agreement with the test data.

EEE LP Turbine Analysis

The EEE LP turbine consists of a 5-stage design employing moderately loaded airfoils and a rather high (25 degrees) endwall slope. The 5-stage design was based in part on results obtained from studies of highly loaded fan turbine technology development at General Electric, and from system studies aimed at minimizing direct operating cost (DOC). The EEE engine LP turbine design is coupled to the HP turbine via a short (3 in.) transition duct. The relatively high bypass ratio (6.8) of the EEE fan section, and subsequent reduced core flow requires high specific energy from the fan-drive (LP) turbine. The design efficiency goals for the LP turbine were 91.1% for the integrated core/low spool (ICLS) test and 91.7% for the flight propulsion system (FPS) at the engine design point (M=0.8, 35,000 ft. altitude ISA). The LPT maximum tip diameter was set by mechanical and configuration control requirements at 46.5 in. The outer wall slope was also limited to 25 degrees (established as a maximum to maintain good aerodynamic performance) through stage 3, transitioning to a cylindrical outer wall at the stage 5 exit.

A mesh system consisting of 10 mesh blocks (1 per blade row for 5 stages) containing 1,660,000 computational cells was assembled.

Design point numerical simulations of the EEE Low Pressure (LP) turbine were performed to permit comparison with 2/3 scale rig test data.[15] The analysis was performed on a Silicon Graphics Power Challenge L multiprocessor computer with 1 GB of main memory. Converged solutions were obtained in a total of 3 hours (wall clock time) using four processors. Note that the turbine simulation was nearly twice as fast as the fan section simulation in spite of the fact that approximately 20% more mesh points were involved. This feature results from the generally favorable pressure gradients involved in the turbine flow, leading to a rapid definition of the boundary layer flow. Conversely, the fan section flow involves predominantly adverse pressure gradients requiring significantly more computation time to resolve. The rapid computation time for the turbine clearly indicates the suitability of the analysis for design cycle studies. In fact, more time was involved in generating suitable meshes than was involved in the aerodynamic analysis itself. Predicted turbine surface static pressure contours are illustrated in Figure 9. This figure illustrates the three-dimensional nature of the blading and the general arrangement of the LP turbine.

A comparison of predicted and experimental spanwise variation of fifth stage exit total pressure and total temperature profiles is given in Figure 10. This preliminary analysis was based on a simple flat inlet profile of total pressure and total temperature and employed the exact blade and endwall definitions provided in the original Master Engine Geometry Database. The correlation between rig test and calculation is excellent in the 20%-80% radial span region. Noticeable discrepancies exist in the near endwall regions. These discrepancies were assumed to be due to the fact that no clearance flows, turbine hub overlap geometry, or shrouded rotor cavity geometries were modeled in this initial prediction.

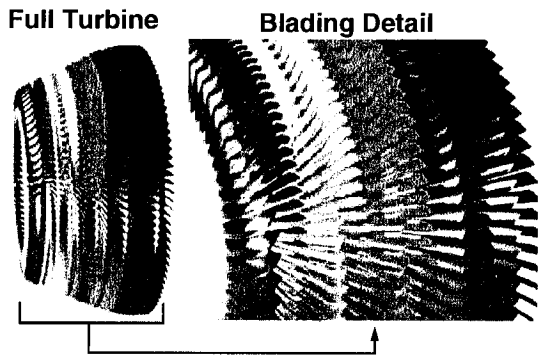

Fig. 9 Predicted surface static pressure contours for EEE LP turbine.

In order to resolve differences between prediction and experiment near the endwalls, several additional calculations were performed to assess the effects of variations in geometry, flow parameters, etc. The variations tested included modifications to the first stage vane setting angle, modifications to the inlet flow profile, and the addition of a shrouded rotor endwall cavity model.

Effect of Variations in First Vane Setting Angle

GE engineers familiar with the actual test rig and EEE engine geometry recommended a 1 degree (open) reset of the LP turbine first stage vane. The effect of the reset on the LP turbine exit spanwise flow profiles is illustrated on Figure 10. A distinct improvement in the predicted total temperature distribution was observed at the turbine exit, particularly near the tip, for the calculation involving the modified geometry. Given this observation, all further calculations were based on the modified first stage vane orientation.

Effect of Variations in Inlet Profile

Several multistage calculations were performed with variations in the first vane input spanwise total pressure, total temperature, and flow angle profile distributions. The profiles are categorized as flat (baseline, essentially no variation across the span except at the tip), boundary layer (BL - 5%/10% (hub/case) thick total pressure deficit at the endwalls), and engine (derived from a simulation of the HP turbine exit flow). An illustration of the spanwise variation of inflow total pressure and total temperature from the three profiles

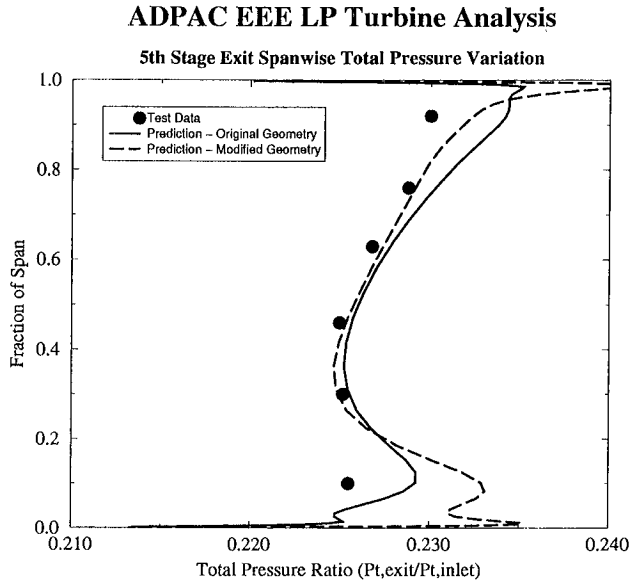

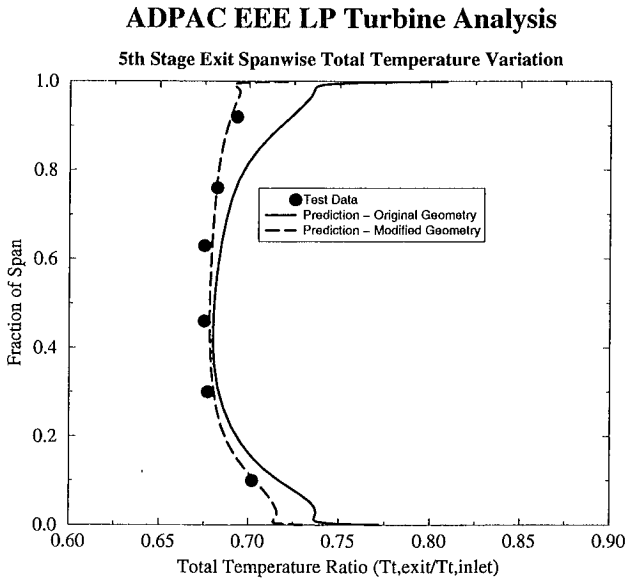

Fig. 10 Comparison of predicted and experimental spanwise variation in fifth stage exit total temperature distributions for EEE LP turbine analyses with variations in first vane reset and endwall modeling.

is given in Figure 11.

Figure 12 illustrates the comparison of predicted and experimental LP turbine exit spanwise total pressure and total temperature profiles for each of the inlet profile variations described above. Note that there is not a significant change in the exit profile total pressure characteristics with variations in inlet profile specification. This is partially due to the fact that each calculation is run to the same exit static pressure ratio. There is some variation in the exit total temperature distributions, although this behavior essentially correlates with the inlet total temperature profile characteristics.

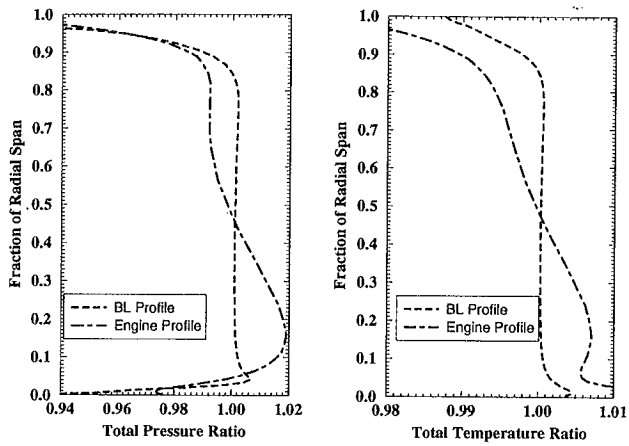

Fig. 11 Comparison of spanwise variation of inflow total pressure and total temperature ratio profiles for profiles for the EEE LP turbine analyses with variations in inlet profile.

Effect of Variations in Endwall Geometry

The final comparison of results involved discrete modeling of the turbine shrouded rotor seal cavities. The calculations described above were all performed using a geometry model based on a smooth, continuous endwall definition. In reality, the endwalls are quite discontinuous and irregular due to the use of shrouded rotors and overlapping geometry, and these irregularities can have a significant impact on the primary gas path flow. Previous experience in predicting flows through compressor seal cavities suggests that the seal cavities themselves can often be modeled using two-dimensional techniques, and then subsequently coupled with the 3-D blade passage flow through averaging techniques similar to a mixing plane. This was the approach adopted in this study to minimize the computational effort involved with modeling this more complicated flow case.

An illustration of the predicted axisymmetric-averaged Mach number contours for the EEE LP turbine with shrouded rotor cavity model is presented in Figure 13. The influence of the cavities would appear to be limited to local regions along the case near the inflow/outflow openings of the cavity.

A summary of the overall performance characteristics due to the variations described above is given in Table 1. In terms of overall performance, variations in inlet profile did not appear to have a significant effect on the predicted mass flow rate, exit total pressure, total temperature, or efficiency for the smooth endwall model. In the cavity endwall model calculations, the differences due to inlet profile were more pronounced. Variations in first vane reset primarily affected the predicted mass flow rate. The 1 degree (open) reset of the first stage vane resulted in an increase in flow of 0.78% for the smooth endwall test case, and an increase of 1.59% for the cavity endwall model test case. Finally, in terms of the effects of variations in

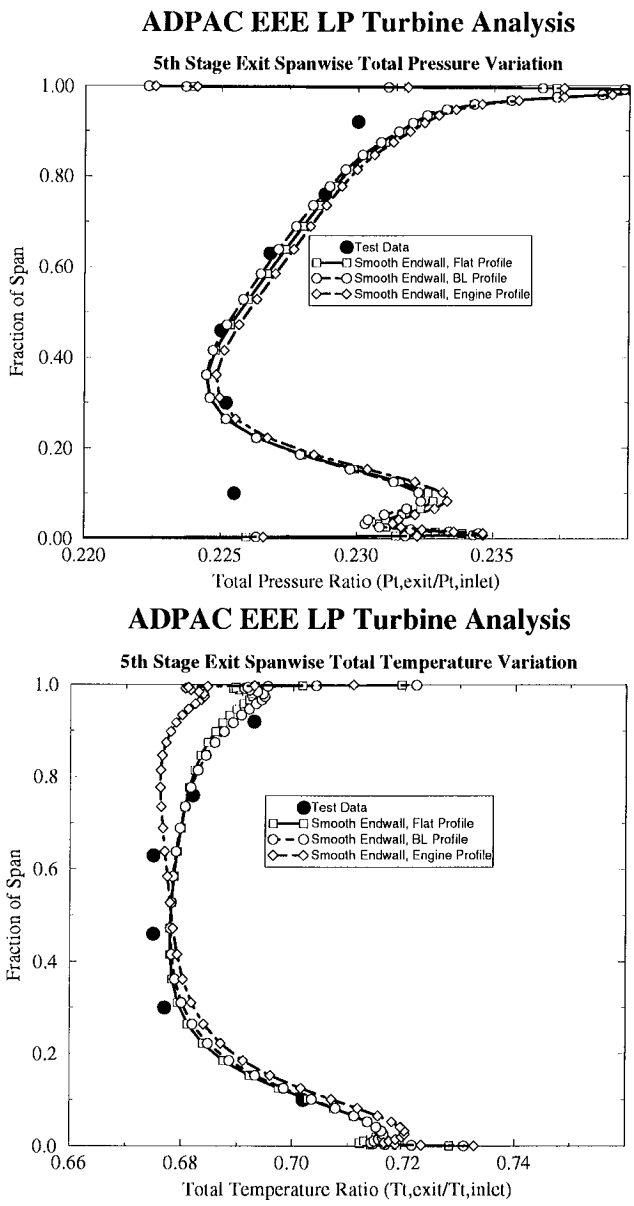

Fig. 12 Comparison of predicted and experimental spanwise variation in fifth stage exit total temperature distributions for EEE LP turbine analyses with variations in inlet profile.

the endwall model, the most prominent characteristics were reductions in predicted mass flow rate and adiabatic efficiency due to the cavity endwall flow model. The reduction in efficiency was quite dramatic - on the order of 3%-5% depending on the test case. One problem encountered during this evaluation was an inability to consistently maintain a constant mass flow from blade row to blade row in the cavity endwall solutions. Typical variations in mass flow from blade row to blade row in the multistage simulations using the smooth endwall model was 0.3%, while the cavity endwall model resulted in blade row to blade row variations as high as 2.0%. The large variation in the cavity flow model was a result of the complicated mixing-

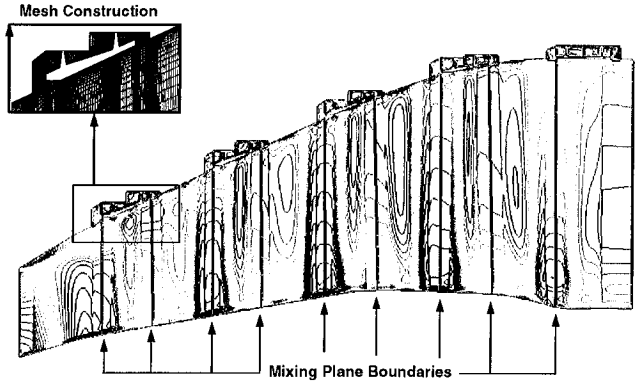

Fig. 13 Illustration of predicted axisymmetric-averaged Mach number contours for the EEE LP turbine with shrouded rotor cavity endwall model.

Inlet Profile Type	First Vane Reset	Endwall Type	Mass Flow (lb/s)	Pt, Exit (psia)	Tt, Exit (deg. R)	Adiabatic Efficiency (Mass-Avg.)
Flat	0	Smooth	67.652	10.299	514.01	91.72%
BL	0	Smooth	67.366	10.292	514.49	91.60%
Engine	0	Smooth	68.228	10.314	512.70	91.99%
BL	1 open	Smooth	67.896	10.308	514.57	91.64%
Flat	0	Cavity	67.146	10.304	526.86	86.74%
BL	0	Cavity	66.705	10.284	522.92	88.27%
BL	1 open	Cavity	67.784	10.316	522.60	88.53%

Notes:
1. Nominal inlet total pressure = 45.0 psia
2. Nominal inlet total temperature = 750 deg. R
3. Approximate variation in computed mass flow from blade row to blade row:
   Smooth Endwall: 0.3%
   Cavity Endwall: 2.0%

Table 1 Comparison of predicted overall performance parameters due to variations in inlet profile, endwall model, and first vane reset for the EEE LP turbine 2/3 scale test rig.

plane arrangement employed to numerically couple the 2-D cavity passage openings with both the upstream and downstream neighboring blade row 3-D mesh systems. Given this large level of mass flow variation, the large predicted efficiency reduction due to the addition of the shrouded rotor cavities should be interpreted qualitatively, not necessarily quantitatively

Off-design component performance *ADPAC* solutions for the LP turbine were compared with GE scaled test rig Block II, Configuration 5 experimental data.[15] *ADPAC* was employed to generate several operating point solutions near the design blade-jet speed ratio ($u/C_o = 0.412$ where u is the turbine inlet mean axial velocity and C_o is the turbine tip speed) for the 2.4 million point LP mesh. The mesh included 2-D shrouded rotor seal geometries. A constant blade-jet speed ratio was set by fixing the inlet-to-exit pressure ratio and solving for the necessary shaft rotational speed. Pressure ratios of 2.0, 3.0 and 4.76 were used for computations and ADPAC data was reduced to enable comparison of equivalent energy extraction, inlet flow function, total-to-total efficiency and total-to-static efficiency. The comparisons are displayed in Figures 14-17.

The predicted trends for equivalent energy extrac-

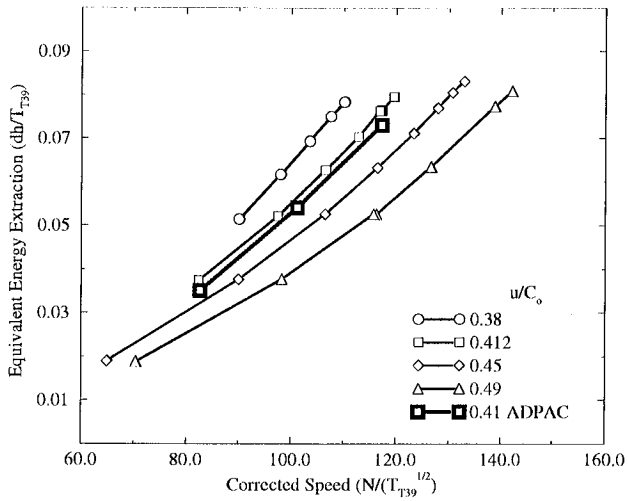

Fig. 14 Comparison of predicted (ADPAC) and measured equivalent energy extraction for the Energy Efficient Engine (EEE) LP turbine.

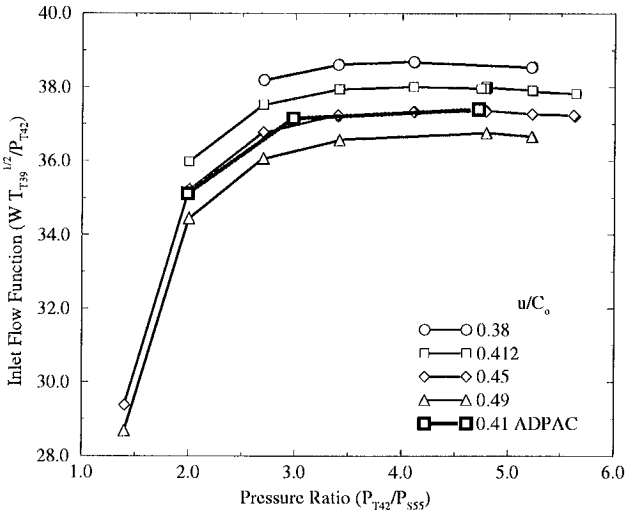

Fig. 15 Comparison of predicted (ADPAC) and measured inlet flow function for the Energy Efficient Engine (EEE) LP turbine.

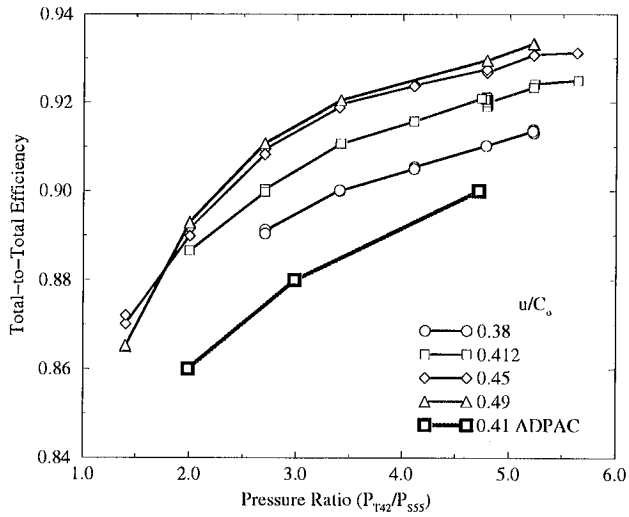

Fig. 16 Comparison of predicted (ADPAC) and measured total to total adiabatic efficiency for the Energy Efficient Engine (EEE) LP turbine.

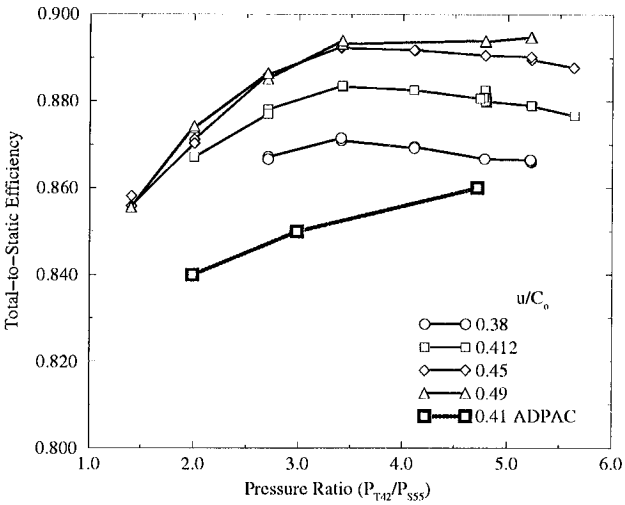

Fig. 17 Comparison of predicted (ADPAC) and measured total to static adiabatic efficiency for the Energy Efficient Engine (EEE) LP turbine.

tion and inlet flow function compare well with the scaled rig test data. The absolute levels of these performance parameters is also predicted reasonably well, in spite of the numerous uncertainties concerning the test vehicle and the data reduction procedures. The predicted trends in efficiency were also captured reasonably well; however, the predicted efficiencies are consistently 2%-4% low. This difference was due, in part, to the modeling of shrouded rotor seal flow, which caused a 3%-5% drop in adiabatic efficiency when compared to the smooth endwall prediction. The discrepancy in efficiency varied considerably based on the numerical method used to compute the efficiency (total temperature, angular momentum change, mass averaging versus area averaging, etc.). The large number of unpublished features of the test rig operation, and the uncertainties associated with the numerical cavity model prohibited timely investigation of this discrepency.

EEE Lobed Exhaust Mixer Analysis

Static scale model tests were conducted to evaluate exhaust system mixers for a high bypass ratio engine as part of the NASA sponsored Energy Efficient Engine Program.[16] Gross thrust coefficients were measured for a series of mixer configurations which included variations in the number of mixer lobes, tailpipe length, mixer penetration, and length. Mixer configuration variables included lobe number, penetration and perimeter, as well as several cutback mixer geometries. Mixing effectiveness and mixer pressure loss were determined using measured thrust and nozzle exit total pressure and temperature surveys. These scaled results provided a data base to aid the anal-

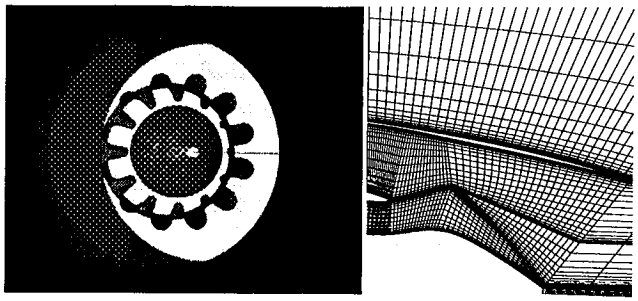

Fig. 18 Illustration of EEE lobed exhaust mixer geometric surfaces and symmetry plane mesh employed during the component validation study (analysis employs one lobe and assumes periodicity from lobe to lobe).

ysis and design/development of the EEE mixed-flow exhaust system. The final EEE Flight Propulsion System (FPS) lobed exhaust mixer employed a scalloped, 12-lobe design based on the results of the extensive rig testing.

Mesh generation was performed using the *GRIDGEN* mesh generation program. A partial geometry database was constructed by NASA during this study and was employed for the EEE LPS simulations described in this section and the following chapter. The geometry is at least representative of the final design, but there remains some uncertainty as to the complete accuracy of the lobed surfaces. In addition, the actual test article employed scallops on the lobes to enhance mixing. Since no detailed information on scallop configuration was available, the cut-outs were not modeled in this study. An illustration of the modeled surfaces of the EEE lobed exhaust mixer is given in Figure 18. The EEE lobed exhaust mixer mesh system along the lobe plane of symmetry is also given in Figure 18. A total of 9 mesh blocks were employed to define the coannular engine flow streams and the external flow stream. An illustration of the mesh system at the mixer plane is given in Figure 18 as well.

A design flow analysis was performed for the EEE lobed exhaust mixer using the *ADPAC* code. Results from the analysis were integrated and qualitatively compared to the test data from the rig test study.[16] Only a qualitative comparison was possible due to uncertainty between the modeled mixer and the geometries described in the rig tests.

Spanwise total temperature profiles at the mixer/nozzle exit are illustrated in Figure 19. Predicted and experimental total temperature ratios are plotted against a normalized nozzle area distribution along several circumferentially spaced arrays spanning a single half-lobe of the mixer. The test data was derived from a study[16] of mixer configurations of varying penetration, area ratio, etc. To validate the mixer predictions, test data was derived from an essentially equivalent mixer (Configuration F3, 12 lobes, 39% penetration) which was tested under the referenced study. In general, the spanwise characteristics of the mixer are qualitatively captured, particularly along the lobe radial peak (Station A on Figure 19 survey. There is some noticeable disagreement between prediction and test at survey Stations D and E. This discrepency is likely due to the fact that the numerical and test mixer geometries were not exactly similar, and also due to the generally accepted observation that the algebraic turbulence model employed in the present analyses is not well suited for temperature mixing problems of this sort.

EEE LP Subsystem Analysis

This section deals with the results of numerical modeling of the Low Pressure (LP) Subsystem of the General Electric (GE) Energy Efficient Engine (EEE). Grid generation for the EEE LP subsystem analysis was based essentially on collecting the individual meshes for the major subcomponents (fan, HP/LP turbines and lobed mixer) employed during the component validation study. The existing fan, quarter-height booster stage, HP turbine, LP turbine, and lobed mixer subsystem component meshes were assembled for this purpose. In addition, new meshes were generated using *GRIDGEN* to model those regions which were not discretized by any of the component validation models. These new regions included the forwardmost flow in the inlet, external flow about the nacelle, and the bypass duct flow between the fan section bypass vane and the lobed exhaust mixer. For computational simplicity, these new regions were modeled in a two-dimensional fashion (the analysis is certainly not limited in this respect), and were computational coupled to the three-dimensional domains using the *ADPAC* mixing plane strategy (see e.g. Figure 20). It should be emphasized that all primary components (blade rows, for example) were still modeled with 3-D mesh systems. The collection and assembly of these meshes resulted in a numerical model of the entire EEE (minus the engine core compressor and combustor). It should be noted that although the high pressure compressor and combustor were not discretely modeled, the influences of these components were approximated by equivalent inflow and outflow boundary conditions. Figure 20 illustrates axisymmetric projections of the resulting EEE mesh/geometry model. The resulting primary mesh for the EEE LP analysis consisted of 74 separate blocks and approximately 6.7 million grid points.

All calculations for the EEE LP Subsystem were performed on parallel computing systems. Timing comparisons for the various computational platforms employed in this study for the EEE LP Subsystem analysis are provided in Table 2.

Overall, the following comments can be made concerning the parallel performance studies:

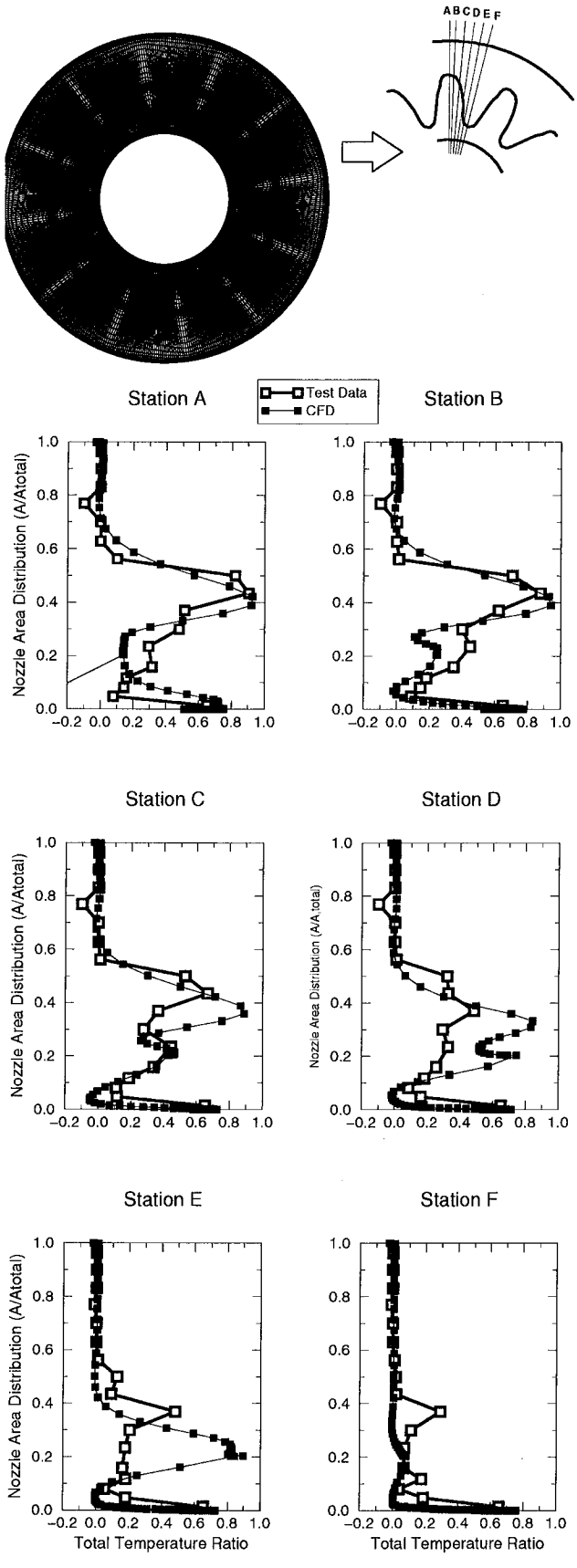

Fig. 19 Comparison of predicted and experimental radial total temperature surveys for the EEE lobed exhaust mixer.

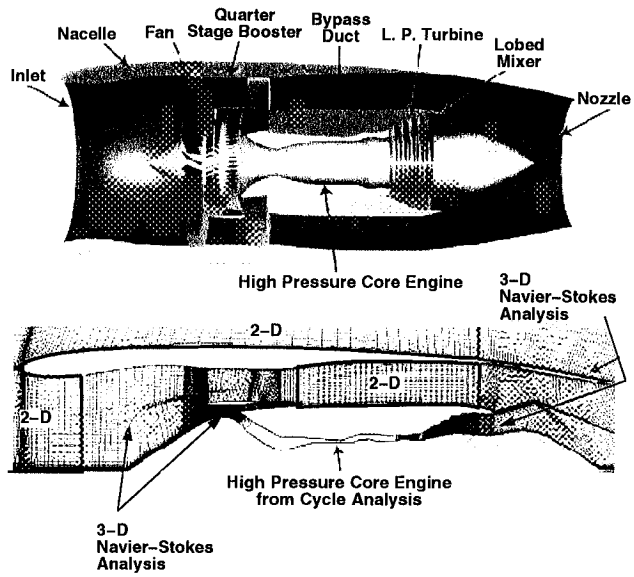

Fig. 20 Axisymmetric projection of Energy Efficient Engine (EEE) Low Pressure (LP) Subsystem analysis component layout and mesh system.

Wall Clock Time Summary
(100 Iterations of EEE/LP Model)

	Coarse Mesh Number of Processors			Fine Mesh Number of Processors		
	8	16	32	8	16	32
LACE						
communication	5380	2139	2707	N/A	23063	–
total solver time	7762	4846	4198	N/A	77427	–
Babbage						
communication	952	403	735	–	–	8763
total solver time	2673	1418	1089	–	–	17518
Davinci						
communication	–	–	–	4617	–	–
total solver time	–	–	–	18122	–	–
Allison SGI Power Challenge						
communication	585	182	N/A	N/A	N/A	N/A
total solver time	1278	673	N/A	N/A	N/A	N/A
Silicon Graphics Origin 2000						
communication	268	153	264	–	–	3105
total solver time	781	403	327	–	–	5528

N/A – not applicable (machine resources insufficient to performing the operation)
LACE: NASA Lewis IBM Rs–6000 cluster
BABBAGE: NASA Ames IBM SP2 cluster
Davinci: NASA Ames SGI cluster

Table 2 Tabulation of parallel computing CPU time estimates for platforms employed for the EEE LP Subsystem analysis (all times given are wall clock time on non-dedicated systems with precautions taken to eliminate outside loading factors).

- Peak processing speed was achieved on a Silicon Graphics Origin 2000 using the SGI MPI 3.0 communication library.
- Estimated turnaround time for a single operating point was estimated to be 10 hours on the SGI Origin 2000 system using 32 processors.
- Load balance was non-optimal for the present mesh configuration. It seems entirely possible that significant improvements in parallel computing efficiency might be achieved through a more

structured specification of mesh block dimensions in the overall problem.

- For the faster systems, parallel computing efficiency was still nearly linear with the addition of more processors. This implies that the problem could still be effectively acclerated if systems with larger numbers of processors (> 100) were available.

The boundary specifications for the EEE LPS analysis were based on a design point engine cycle analysis derived from results from the NEPP computer code. Note that for this set of results, the HP turbine (normally considered a core, or HP subsystem component) was employed in the CFD model to permit a more reasonable specification of the spanwise flow profiles entering the LP turbine. Subsequent large-scale simulations of the LP Subsystem did not employ the CFD representation of the HP turbine as it was ultimately demonstrated that the LP turbine performance is relatively insensitive to inlet flow profile.

EEE LPS Shaft Power Balance

An important aspect of engine simulation, compared to component simulation, is that the mating of components often involves both aerodynamic *and* mechanical couplings. This concept is illustrated for both single-spool and twin-spool gas turbine engines in Figure 21. This concept is commonly employed in cycle deck analyses (e.g. *NEPP*) for components connected by a common shaft. The same concept can be applied to larger-scale simulations by providing the appropriate aerodynamic consistency between components (mass flow, etc.) as well as equating the overall power requirements for common shaft-mounted components. This balance was iteratively achieved in the present simulation through an iterative procedure which employed shaft rotational speed as the means of achieving the desired shaft power balance.

A series of solutions for the EEE/LP Subsystem was obtained for fixed shaft rotational speeds. For each shaft speed, computed power and torque for the rotating components were integrated for the rotating components of both the LP turbine and fan/booster-stage assemblies. Differences between the computed power/torque requirements for the fan and LP turbine assemblies were then employed to estimate a new shaft speed for the subsequent solution. Simple physical reasoning suggests that if there is power excess, then the shaft speed should increase, and if there is a power deficit, then the shaft speed should decrease. A simple linear interpolation was employed to estimate the updated shaft speed based on the integrated results from two previous solutions.

A portion of the iterative history of the ADPAC EEE LP shaft power balance is given in Table 3. As the shaft speed was reduced, the power required by the

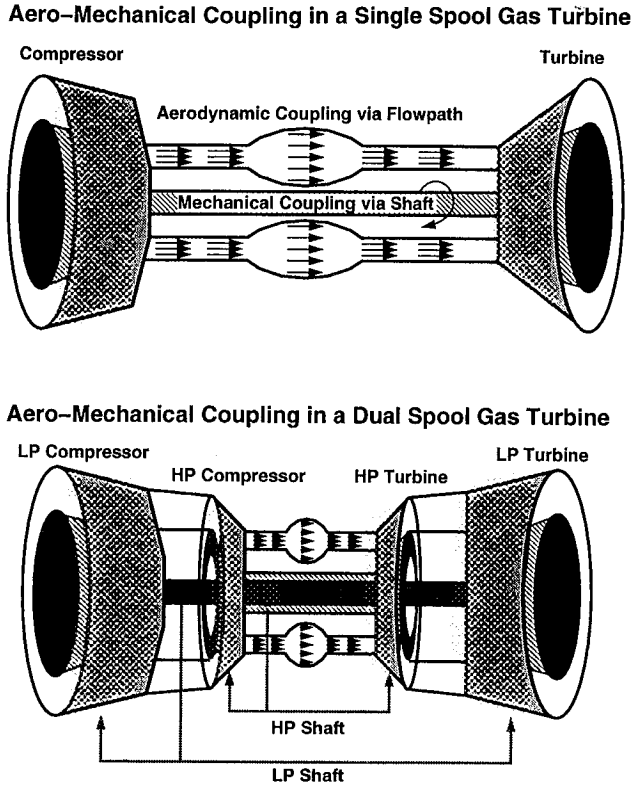

Fig. 21 Illustration of aerodynamic/mechanical balance required for single-spool and twin-spool gas turbine engines.

fan was reduced, while the power provided by the LP turbine increased. Eventually, these two power levels were essentially identical. The balance was deemed converged when the power balance was within 1%. Note that in spite of the changes to the LP system, the HP turbine power was relatively constant. This is essentially a result of the fact that the core performance was fixed during the shaft power balance procedure. The absolute power levels must be interpreted with the limitations of the CFD analysis in mind. The analysis was performed with a constant specific heat, when in fact, given the range of temperatures in the machine, the specific heat actually varies up to 5%. In addition, parasitic losses in the compressor (endwall leakages, cavity flows, etc.) have not been included in the analysis. The shaft power balance also assumes a 100% transmission efficiency (no bearing losses).

Core Cycle Boundary Specification

Following the completion of the effort to develop an LP Subsystem shaft power balance computational procedure, the logical next step in the LP Subsystem analysis was to couple the 3-D ADPAC predictions with a lower order (cycle deck) analysis of the core component performance. This coupling is consistent with the "zooming" philosophy inherent in the NPSS

ADPAC Solution (Fixed RPM/Fixed Core, ft-lbf/sec)

Shaft RPM	Fan	LP Turbine	HP Turbine
3507	8,622,000	6,947,200	12,634,000
3407	8,028,000	7,002,600	12,619,000
3250	7,522,300	7,301,400	12,557,000
3200	7,243,100	7,322,700	12,547,000

NEPP Solution (Design Point)

Shaft RPM	Fan	LP Turbine	HP Turbine
3538.5	8,182,000	8,182,000	11,625,300

Table 3 Tabulation of coarse mesh EEE LP Subsystem shaft power balance iterative results.

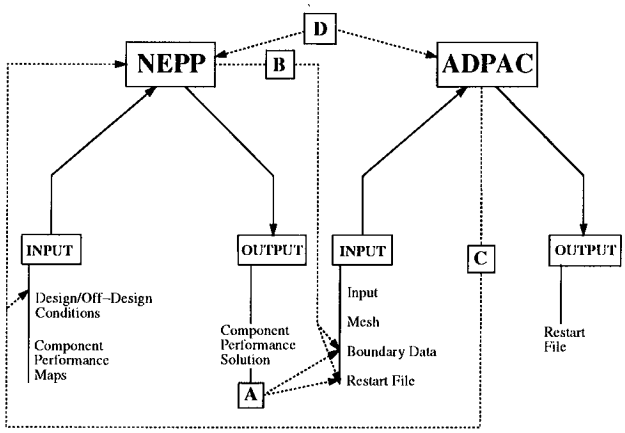

ADPAC/NEPP Interaction

A. Use NEPP output to create ADPAC Boundata and Restart files
   1. No direct link between NEPP and APAC
   2. NEPP output file updates EXIT and INLET conditions and RPM boundata file
   3. NEPP output file creates ADPAC restart file to aid in "start-up" process
B. Create coding changes in NEPP to perform A
C. Use SYSTEM call in ADPAC boundata file to run NEPP from ADPAC
D. Use front-end script to control NEPP-ADPAC interations

Fig. 22 Coupled ADPAC/NEPP analysis schematic data flow representation.

system architecture. In the present application, the core cycle model was based on predictions from the *NEPP* code. In order to incorporate the *NEPP* results in a systematic fashion, the various interactions between the NEPP core model and the *ADPAC* LP Subsystem model must be addressed. One interpretation of these interactions is outlined schematically in Figure 22. The specifications required from NEPP for the ADPAC analysis are an estimate of the core compressor inlet flow (represented initially by a static pressure which is used to set the flow in the ADPAC solution), and a specification of the HP turbine inlet total pressure and total temperature profiles describing the flow out of the EEE combustor. The specifications required from the ADPAC analysis for the NEPP analysis include the core compressor inlet total pressures, temperature and velocities (which result from the CFD analysis of the fan section). Intertwined in this cross specification is the fact that the LP shaft RPM may change as the overall solution evolves, and the level and frequency by which the exchanged boundary data between the two analyses occurs may be critical.

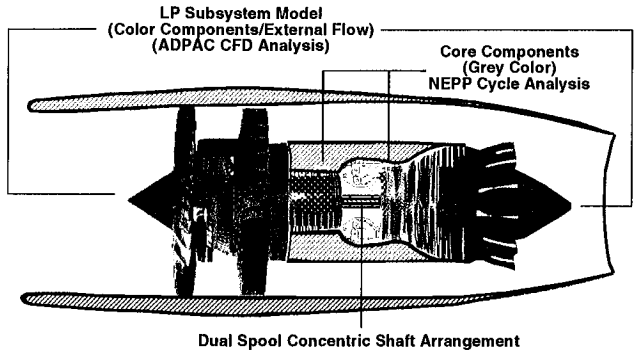

Fig. 23 Illustration of coupled ADPAC/NEPP prediction for the EEE LP Subsystem (color contours indicate predicted static pressure ratio: red-10.0, blue-0.36, grey scale components are represented by the NEPP cycle analysis).

The computational system resulting from the combined *NEPP/ADPAC* computational procedure is illustrated graphically in Figure 23. Since this procedure was designed for demonstration purposes, the coupling between the *ADPAC* and *NEPP* analyses was controlled by a UNIX shell script which sequentially applied the analyses in an iterative fashion. Following the application of each analyses, the appropriate flow information was extracted from output files by hardwired programs developed specifically for these two codes, and based specifically on the format of the output for each codes. This was, unfortunately an inflexible system, but did have the advantage that it could be assembled rather quickly to demonstrate the overall concept.

A solution for the EEE/LP Subsystem using the coupled *ADPAC/NEPP* solution strategy was obtained for the design operating point. Problems encountered during the initial tests of the solution procedure were traced to excessive variations in the boundary specifications during the initial phases of the calculations. These excursions were modulated using a simple under-relaxation procedure. The behavior of the overall solution procedure was then relatively stable, albeit very slow. Individual *ADPAC solutions* acquired during the iterative cycle can take up to 8 hours on a parallel system, with some 10-20 iterations required to achieve complete coupling between the ADPAC and NEPP analyses.

It should be noted that the present demonstration did not employ the LP shaft power balance procedure which would be essential to complete the coupled solution procedure. At this point, a demonstration of the concept was considered of primary importance. The capability demonstrated through this exercise validates the NPSS primary objective of "*zooming*", and can hopefully lead to further research in employing this type of analysis for future gas turbine engine studies.

Concluding Remarks

Computational Fluid Dynamics (CFD) analysis of the complete Low Pressure (LP) Subsystem of the General Electric Energy Efficient Engine (EEE) was demonstrated. This study identified several important topical areas to consider in the planning and execution of large-scale simulations of complete gas turbine engine propulsion systems. The topical areas include geometry manipulation, mesh generation, solution initialization, application of parallel computing, full-scale engine simulation, and interpretation of computational results. Detailed analysis of the procedures and predicted results yielded the following considerations:

- Some form of geometry manipulation is essential to permit realistic representation of industry gas turbine engine designs
- The effects of secondary flow systems (leakage paths, cooling flows, etc.) on primary gas flowpath performance are significant and require further modeling research to permit valid simulations of engine environment flows.
- Improvements to the mixing plane solution strategy (addition of deterministic stresses, nonreflecting procedures) may aid convergence and solution integrity.
- Access to larger scale (> 32 processors) parallel cluster systems would permit more rapid analysis.

Acknowledgements

The work described in this paper was supported under the NASA High Performance Computing and Communication Program (HPCCP), contract NAS3-27394, Task 13.

References

[1]Fagan, J. R. and Hall, E. J., "Mixing Mechanisms in Multistage Compressors," *Advanced Turbomachinery Design*, 1997.

[2]Hall, E. J., "Aerodynamic Modeling of Multistage Compressor Flowfields-Part 1: Analysis of Rotor/Stator/Rotor Aerodynamic Interaction," ASME Paper 97-GT-344, Jun. 1997.

[3]Hall, E. J., "Aerodynamic Modeling of Multistage Compressor Flowfields-Part 2: Modeling Deterministic Stresses," ASME Paper 97-GT-345, Jun. 1997.

[4]Klann, J. L. and Snyder, C. A., "NEPP Programmers Manual (NASA Engine Performance Program) Volume 1. Technical Description," NASA TM 106575, Sep. 1994.

[5]Barber, T., Choi, T., McNulty, G., Hall, E., and Delaney, R., "Preliminary Findings in Certification of ADPAC," AIAA Paper 94-2240, Jun. 1994.

[6]Hall, E. J. and Delaney, R. A., "Investigation of Advanced Counterrotation Blade Configuration Concepts for High Speed Turboprop Systems: Task VII - ADPAC User's Manual," NASA CR 195472, Jul. 1995.

[7]Jameson, A., Schmidt, W., and Turkel, E., "Numerical Solutions of the Euler Equations by Finite Volume Methods Using Runge-Kutta Time-Stepping Schemes," AIAA Paper 81-1259, 1981.

[8]Adamczyk, J. J., Celestina, M. L., and Beach, T. A., "Simulation of Three-Dimensional Viscous Flow Within a Multistage Turbine," ASME Paper 89-GT-152, 1989.

[9]Arnone, A. A., Liou, M. S., and Povinelli, L. A., "Multigrid Time-Accurate Integration of Navier-Stokes Equations," AIAA Paper 93-3361-CP, 1993.

[10]Baldwin, B. S. and Lomax, H., "Thin Layer Approximation and Algebraic Model for Separated Turbulent Flows," AIAA Paper 78-257, 1978.

[11]"MPI: A Message-Passing Interface Standard," *International Journal of Supercomputing Applications*, Vol. 8, No. 3/4, 1994.

[12]et. ãl., J. S., "The Gridgen 3D Multiple Block Grid Generation System." Final Report WRDC-TR-90-3022, Jun. 1990.

[13]Anderson, D. A., Tannehill, J. C., and Pletcher, R. H., *Computational Fluid Mechanics and Heat Transfer*, 1984.

[14]Cline, S. J., Halter, P. H., Kutney, J. T., and Sullivan, T. J., "Energy Efficient Engine: Fan and Quarter-Stage Component Performance Report," NASA CR 168070, Jan. 1983.

[15]Bridgeman, M. J., Cherry, D. G., and Pedersen, J., "NASA/GE Energy Efficient Engine Low Pressure Turbine Scaled Test Vehicle Performance Report," NASA CR 168290, Jul. 1983.

[16]Rowe, R. K. and Kuchar, A. P., "Energy Efficient Engine (E^3) Scaled Mixer Performance Report - Final Report," NASA CR 167947, Nov. 1982.

REPORT DOCUMENTATION PAGE

Form Approved
OMB No. 0704-0188

1. AGENCY USE ONLY (*Leave blank*)	2. REPORT DATE	3. REPORT TYPE AND DATES COVERED
	July 1998	Technical Memorandum

4. TITLE AND SUBTITLE

Energy Efficient Engine Low Pressure Subsystem Aerodynamic Analysis

5. FUNDING NUMBERS

WU–509–10–11–00

6. AUTHOR(S)

Edward J. Hall, Robert A. Delaney, Sean R. Lynn, and Joseph P. Veres

7. PERFORMING ORGANIZATION NAME(S) AND ADDRESS(ES)

National Aeronautics and Space Administration
Lewis Research Center
Cleveland, Ohio 44135–3191

8. PERFORMING ORGANIZATION REPORT NUMBER

E–11234

9. SPONSORING/MONITORING AGENCY NAME(S) AND ADDRESS(ES)

National Aeronautics and Space Administration
Washington, DC 20546–0001

10. SPONSORING/MONITORING AGENCY REPORT NUMBER

NASA TM—1998-208402

11. SUPPLEMENTARY NOTES

Prepared for the 34th Joint Propulsion Conference and Exhibit cosponsored by AIAA, ASME, SAE, and ASEE, Cleveland, Ohio, July 13–15, 1998. Edward J. Hall, Robert A. Delaney, and Sean R. Lynn, Allison Engine Company, Indianapolis, Indiana 46241; Joseph P. Veres, NASA Lewis Research Center. Responsible person, Joseph P. Veres, organization code 2900, (216) 433–2436.

12a. DISTRIBUTION/AVAILABILITY STATEMENT

Unclassified - Unlimited
Subject Categories: 07 and 02 Distribution: Nonstandard

This publication is available from the NASA Center for AeroSpace Information, (301) 621–0390.

12b. DISTRIBUTION CODE

13. ABSTRACT ***(Maximum 200 words)***

The objective of this study was to demonstrate the capability to analyze the aerodynamic performance of the complete low pressure subsystem (LPS) of the Energy Efficient Engine (EEE). Detailed analyses were performed using three-dimensional Navier-Stokes numerical models employing advanced clustered processor computing platforms. The analysis evaluates the impact of steady aerodynamic interaction effects between the components of the LPS at design and off-design operating conditions. Mechanical coupling is provided by adjusting the rotational speed of common shaft-mounted components until a power balance is achieved. The Navier-Stokes modeling of the complete low pressure subsystem provides critical knowledge of component aero/mechanical interactions that previously were unknown to the designer until after hardware testing.

14. SUBJECT TERMS

System model; Computer simulation; CFD; Turbofan engine; Flow; Performance; Aerodynamics

15. NUMBER OF PAGES

22

16. PRICE CODE

A03

17. SECURITY CLASSIFICATION OF REPORT	18. SECURITY CLASSIFICATION OF THIS PAGE	19. SECURITY CLASSIFICATION OF ABSTRACT	20. LIMITATION OF ABSTRACT
Unclassified	Unclassified	Unclassified	